Cavity Design and Beam Simulations for the APS RF Gun

Advanced Photon Source

Michael Borland—15 November 1991

An earlier note discussed the preliminary design of the 1-1/2 cell RF cavity for the APS RF gun. This note describes the final design, including cavity properties and simulation results from the program `rfgun`[7].

The basic idea for the new design was that the successful SSRL design [1, 2, 3] could be improved upon by reducing fields that had nonlinear dependence on radius. As discussed previously, this would reduce the emittance and produce tighter momentum and time distributions. In addition, it was desirable to increase the fields in the first half-cell relative to the fields in the second half-cell, in order to allow more rapid initial acceleration, which would reduce the effects of space charge. Both of these goals were accomplished in the new design.

1 Cavity Design

In the previous note, I discussed how it was necessary to increase the distance between the cathode and the center of the second cell in order to allow the use of a higher accelerating gradient in the first cell. Two designs were given, one with a 4 mm cathode offset and another with a 6 mm cathode offset. Simulations with `rfgun` indicated that the later design gave superior performance, and hence the design presented here has a 6 mm cathode offset.

The design is shown in Figure 1. Table 1 gives the geometry of the design. For arcs of circles, z and r refer to the center of the arc. All arcs are connected by vertical or horizontal lines only, as required to make a continuous curve. The second cell (i.e., that part to the right of point 12) is symmetric about the point labeled 20, except for the elongated exit beam tube.

In the previous note, I gave the off-axis field expansion for the RF fields in the gun cavity, and stated that the amount of nonlinearity could be gauged by examining two functions, defined by

$$T_1(z) = \frac{R_c^2}{8 \times \max(E_z(z, r=0))} \left[\partial_z^2 + k^2\right] E_z(z, r=0) \tag{1}$$

and

$$T_2(z) = \frac{R_c^2}{8 \times \max(E_z(z, r=0))} \left[\partial_z^3 + k^2 \partial_z\right] E_z(z, r=0), \tag{2}$$

where R_c is the cathode radius. T_1 is proportional to the magnitude at $r = R_c$ of the r^3 term of B_ϕ and the r^2 term of E_z terms relative to, respectively, the r^1 term of B_ϕ and the constant term of E_z. Similarly, T_2 measures the r^3 term of E_r relative to the linear term, at the cathode radius. T_1 is related primarily to degradation of the momentum spectrum, while T_2 is related primarily to degradation of the emittance.

Figure 2 shows various quantities related to the RF fields in the new cavity. In addition to the on-axis longitudinal electric field, the Figure shows the radial field at the cathode radius, reconstructed from off-axis expansions to third and fifth order in r. Note that the third and fifth order expansions are virtually identical, which attests to the extent to which nonlinear fields have been suppressed. Finally, the Figure compares T_1 and T_2 for the new cavity and the SSRL cavity.

2 Cavity Properties

The cavity calculations, including the field calculations shown above, have been done using URMEL[4] and checked with SUPERFISH[5]. The first cell was tuned to 2894.4 MHz and the second cell to 2872.4 MHz, the approximate values required to obtain 2856 MHz when the effects of waveguide and coupling cell apertures are considered[6].

Table 2 lists parameters of the first and second cells, treated individually, using values from URMEL (for which a finer mesh can be used than in SUPERFISH). The shunt impedance is defined as $V_i^2/(2P_i)$, where $V_i = \int_{cell} E_z(z)dz$. E_{ps} is the peak surface field, E_c is the peak field at the cathode, and E_{pi} is the peak, on-axis longitudinal electric field in the i^{th} cavity. K_i is defined as U_i/E_{pi}^2.

For whole-gun calculations, it is necessary to assume some value of the excitation ratio, defined as $\alpha = E_{p2}/E_{p1}$. The SSRL gun has $\alpha \approx 3$. The APS gun has been designed to have $\alpha \approx 1.7$. This gives the necessary momentum vs exit-time relationship for magnetic compression (see below).

The Q of the cavity is given by[1]

$$Q = Q_2 \frac{1 + \frac{K_1}{K_2\alpha^2}}{1 + \frac{1}{\alpha^2}\frac{K_1 Q_2}{K_2 Q_1}}. \tag{3}$$

Using the parameters given in the table, I obtain 15946 for the Q of the $\pi/2$ structure mode.

Similarly, one can express E_{p2} in terms of the total power, P, dissipated in the cavity walls, using

$$E_{p2} = \sqrt{\frac{Q_2}{\omega K_2(1 + \frac{1}{\alpha^2}\frac{K_1 Q_2}{K_2 Q_1})}}\sqrt{P}, \tag{4}$$

giving $E_{p2} = 58.3(MV/m/MW^{\frac{1}{2}})\sqrt{P}$. For the SSRL gun, the coefficient was 80. The decrease reflects the decrease in shunt impedance resulting from the longer RF gaps in both the first and second cell of the new gun. However, with a more uniform field level in the first and second cells, the new design produces more energetic beams for lower values of E_{p2}.

3 rfgun Simulation Results

The program `rfgun`[7] was used as part of the design process, and has been used to simulate the APS RF gun in the absence of space-charge effects. (Preliminary calculations of the effect of space-charge in the first cell have been done using the program MASK[8]. These are discussed below.)

Figures 3 and 4 show various gun performance parameters as a function of E_{p2}, for cathode radii of 2 mm and 3 mm. The parameters in Figure 3 are for a $\pm 5\%$ momentum spread, defined by

$$p \geq p_{max}\frac{1-f}{1+f}, \tag{5}$$

where $f = 0.05$. I will refer to the beam so defined as the "useful beam". Q_b is the charge per bunch divided by the current density, J, which accounts for 35 to 50 % of the charge exiting the gun (the fraction is higher for higher E_{p2}). $\epsilon_x = \epsilon_y$ is the RMS geometric emittance, defined by

$$\epsilon_x = \sqrt{\langle x^2\rangle\langle x'^2\rangle - \langle x'x\rangle^2}. \tag{6}$$

B_T is the transverse brightness, which I define as[1]

$$B_T = \frac{2Q_b}{\epsilon_x \epsilon_y}. \tag{7}$$

To date, MASK simulations have been done for the first cell, for $E_{p2} = 70$ MV/m, and for a 2 mm cathode radius only. For zero current density and for f=0.05, the emittance predicted by MASK is about 20% larger than that predicted by `rfgun`. At $J = 50 A/cm^2$, the emittance is about 80% of the zero-current-density emittance (a paradoxical result that comes about because a given momentum interval contains a different initial phase interval for different current densities). At zero current density, MASK predicts an RMS radial coordinate of 1.2 mm, an RMS radial divergence of 10.3 mrad, and a bunch length of 13.1 ps. At $J = 50 A/cm^2$, these become, respectively, 1.4 mm, 16.9 mrad, and 13.9 ps.

A future report will give results of MASK simulations of the full gun, over a wider parameter space. Results[1] of MASK simulations for the SSRL gun were that the emittance doubled when the current density was increased from essentially zero to 80 A/cm^2 for a cathode radius of 3 mm. The effect of space-charge in the APS RF gun should be less than this, since the fields at the cathode are greater than in the SSRL gun. The preliminary simulations reported in the last paragraph confirm this expectation.

Figure 4 shows parameters for the entire beam and for the cavity. P_1 and P_2 are the beam power divided by the current density exiting, respectively, the first and second cells in the forward direction. P_{bb} is the current-density-normalized beam power that returns to hit the plane z=0 (i.e., the plane of the cathode); the subscript "bb" stands for back-bombardment. P_w is the power dissipated in the cavity walls.

Like the SSRL gun, the APS gun is designed to be matched when the beam power is three times the cavity wall power (i.e., the normalized load impedance of the cavity without beam is $\beta_o \approx 4$). Neglecting those few particles that are lost on apertures inside the gun, the total power into particles is $JP_2 + JP_{bb}$, and thus the current density at which the matched condition holds in the steady-state is

$$J_m = \frac{3P_w}{P_2 + P_{bb}}. \tag{8}$$

Figure 5 shows J_m and other results for the matched condition. The charge in each bunch of the useful beam is $Q_m = J_m Q_b$ and the transverse brightness is $B_{T,m} = J_m B_T$. The total RF power required is $P_{RF,m} = P_w + J_m(P_2 + P_{bb})$.

One sees that considerable RF power is required to operate in the matched condition at higher values of E_{p2}. In fact, more RF power is required than indicated in the Figure, since I have not included losses in the side-coupling cell. These losses will inevitably occur as net power flows into the first cell from the second cell via the coupling cell to supply power to accelerate the beam. Future work will include a treatment of this problem. Experiments done at SSRL indicate that the actual power requirements may be 50% higher than indicated in the Figure.

Note, however, that it is not *necessary* to run the gun in the matched condition. This is only the most efficient use of the RF power. If the current density is decreased below that required for a match, then the efficiency decreases, but so does the input RF power required to achieve a given value of E_{p2}. Neglecting effects of the side-coupling cell, the input RF power required for a current density of J is

$$P_{RF} = \frac{P_w}{4\beta_o}\left(\beta_o + 1 + \frac{J}{J_m}(\beta_o - 1)\right)^2. \tag{9}$$

To give a more complete picture of the beam from the gun, I end this section with transverse phase-space plots for several different values of E_{p2}. These appear in Figure 6.

4 Bunch Compression Results

After exploring various options for magnetic bunch compression[1], I have concluded that an alpha-magnet-and-drift system is very difficult to beat in terms of both bunch compression and preservation of the transverse emittance. In this section, I report on preliminary results for a bunch-compressing beamline consisting of an alpha-magnet and a 2 meter drift. A more detailed analysis, including transverse effects, quadrupole focusing, and discussion of alternatives, will appear in the future.

The time-of-flight in a drift space of length L is

$$\Delta t_d = \frac{L}{\beta c}, \tag{10}$$

while the time-of-flight in an alpha-magnet is[1]

$$\Delta t_\alpha = \frac{K_\alpha}{\beta c}\sqrt{\frac{\beta\gamma}{\nabla B}}, \tag{11}$$

where $K_\alpha = 1.91655\text{m}\sqrt{\text{G/cm}}$ and ∇B is the alpha-magnet gradient. Given the momentum, $p = \beta\gamma$, and the time of exit, t_{ex}, for any particle, the time-of-arrival at the end of the drift-and-alpha-magnet system is

$$t_a = t_{ex} + \Delta t_d + \Delta t_\alpha. \tag{12}$$

The program `alpha_opt` uses this equation to find the optimum value of ∇B for a given set of (t_{ex}, p) pairs. For present purposes, I define "optimum" to mean that condition where the spread in t_a is minimized. For any value E_{p2}, a set of (t_{ex}, p) pairs can be generated by running `rfgun`. Data for E_{p2} between 50 and 80 MV/m, and a cathode radius of 3 mm, is shown in Figure 7, where I present histograms of the time and momentum distributions as well as (t_{ex}, p) for individual simulation particles.

Figure 8 shows the results of running `alpha_opt` on the data of the previous Figure. The best results are achieved for $E_{p2} = 60\text{MV/m}$, a result of choosing 2 meters for the drift-length. (Note that the optimal drift length for the lowest emittance beam ($E_{p2} = 70\text{MV/m}$) is about 8 meters, which is impractically long.)

Figure 9 shows various parameters before and after compression. Δt_i and Δt_f are, respectively, the initial and final bunch lengths. Also, shown are the alpha-magnet gradient and x_{max}, the maximum extent of the trajectory inside the alpha-magnet.

5 Acknowledgements

I wish to thank Eiji Tanabe of AET for helpful discussion and ideas about the new design.

References

[1] M. Borland, *A High-Brightness Thermionic Microwave Electron Gun*, Stanford University Ph.D. Thesis, 1991.

[2] E. Tanabe, *et. al.*, "A 2-MeV Microwave Thermionic Gun", SLAC-PUB-5054.

[3] M. Borland, *et. al.*, "Performance of the 2 MeV Microwave Gun for the SSRL 150 MeV Linac", in *Proceedings of the Linear Accelerator Conference*, September, 1990. Also SLAC-PUB-5333.

[4] U. Laustroer, *et. al.*, "URMEL and URMEL-T User Guide", DESY-M-83-03, February 1987.

[5] K. Halbach, R. F. Holsinger, "SUPERFISH–A Computer Program for Evaluation of RF Cavities with Cylindrical Symmetry, *Particle Accelerators*, **7**:213-222, 1976.

[6] E. Tanabe, private communication.

[7] M. Borland, "`rfgun`: A Program to Simulate RF Guns", SSRL ACD-Note 78, March 13, 1991.

[8] A. T. Drobot, *et. al.*, "Numerical Simulation of High Power Microwave Sources", *IEEE Trans.*, **32**: 2733-7, 1985.

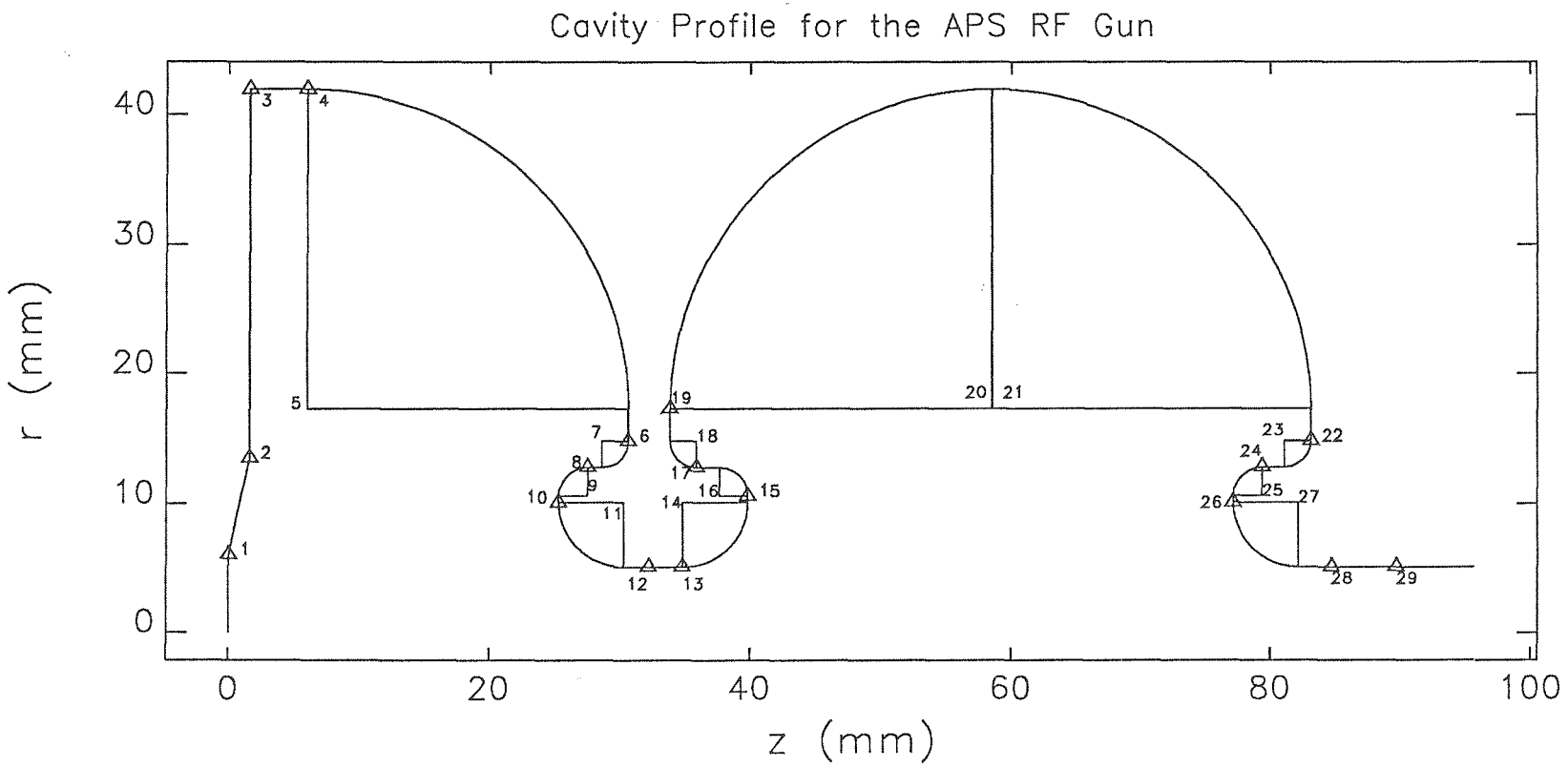
Cavity Profile for the APS RF Gun
r (mm)
z (mm)
0
10
20
30
40
0
20
40
60
80
100
1
2
3
4
5
6
7
8
9
10
11
12
13
14
15
16
17
18
19
20
21
22
23
24
25
26
27
28
29

Figure 1

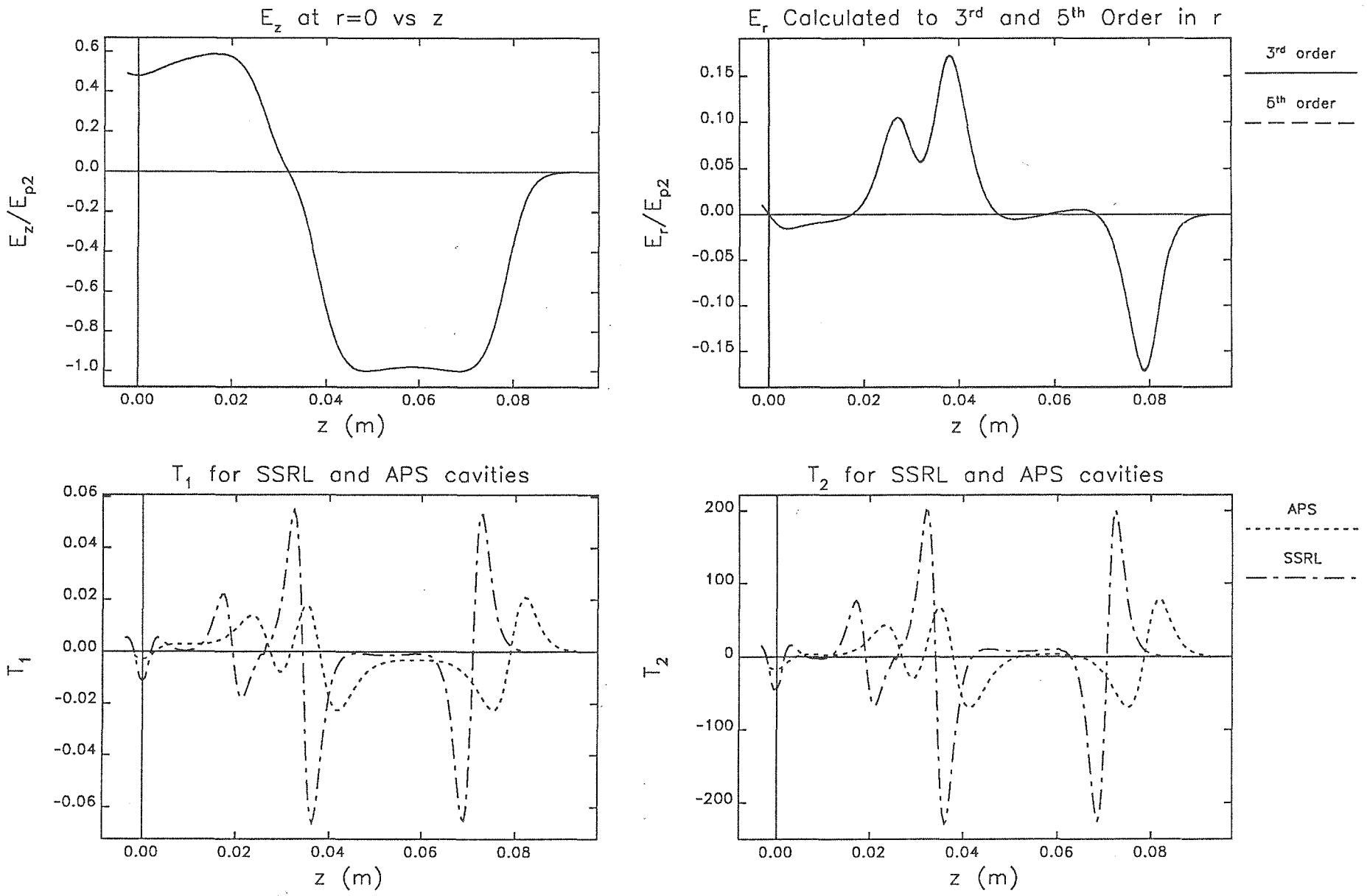
E_z at r=0 vs z
E_z/E_{p2}
z (m)
E_r Calculated to 3rd and 5th Order in r
E_r/E_{p2}
3rd order
5th order
T_1 for SSRL and APS cavities
T_1
T_2 for SSRL and APS cavities
T_2
APS
SSRL

Figure 2

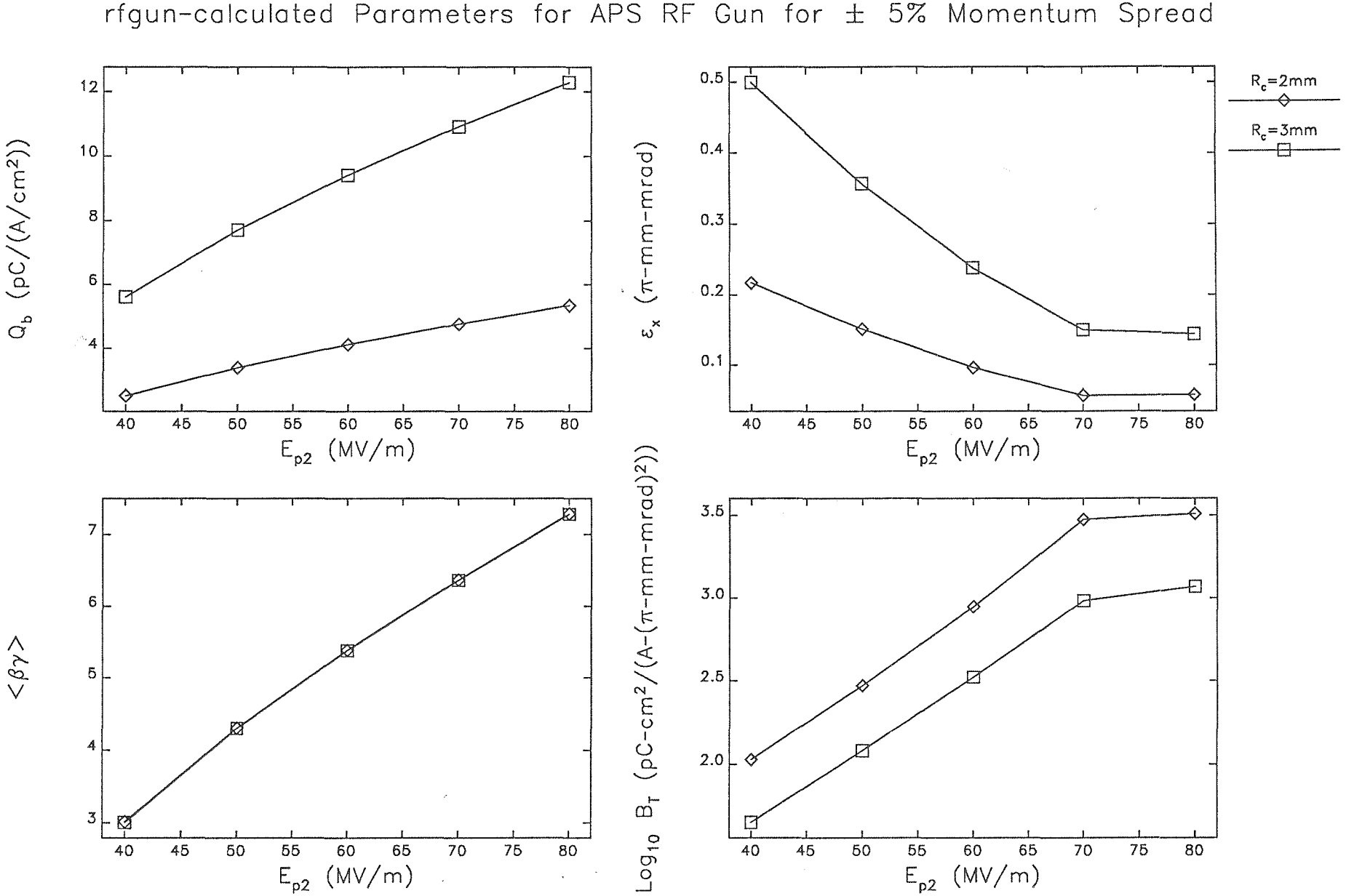
rfgun-calculated Parameters for APS RF Gun for ± 5% Momentum Spread
Q_b (pC/(A/cm^2))
E_{p2} (MV/m)
ε_x (π-mm-mrad)
$<\beta\gamma>$
Log_{10} B_T (pC-cm^2/(A-(π-mm-mrad)^2))
R_c=2mm
R_c=3mm

Figure 3

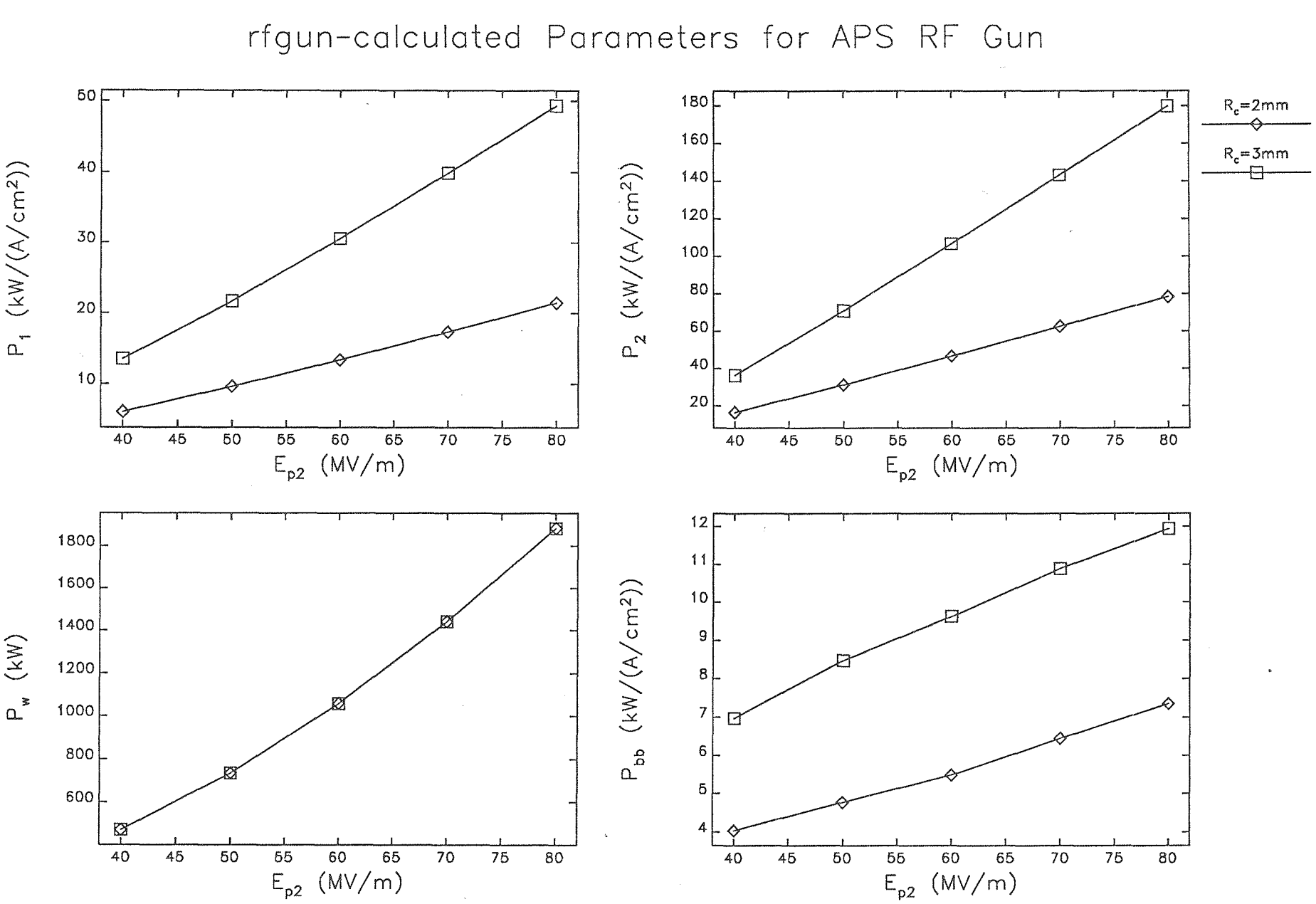
rfgun-calculated Parameters for APS RF Gun
P1 (kW/(A/cm2))
Ep2 (MV/m)
P2 (kW/(A/cm2))
Ep2 (MV/m)
Rc=2mm
Rc=3mm
Pw (kW)
Ep2 (MV/m)
Pbb (kW/(A/cm2))
Ep2 (MV/m)

Figure 4

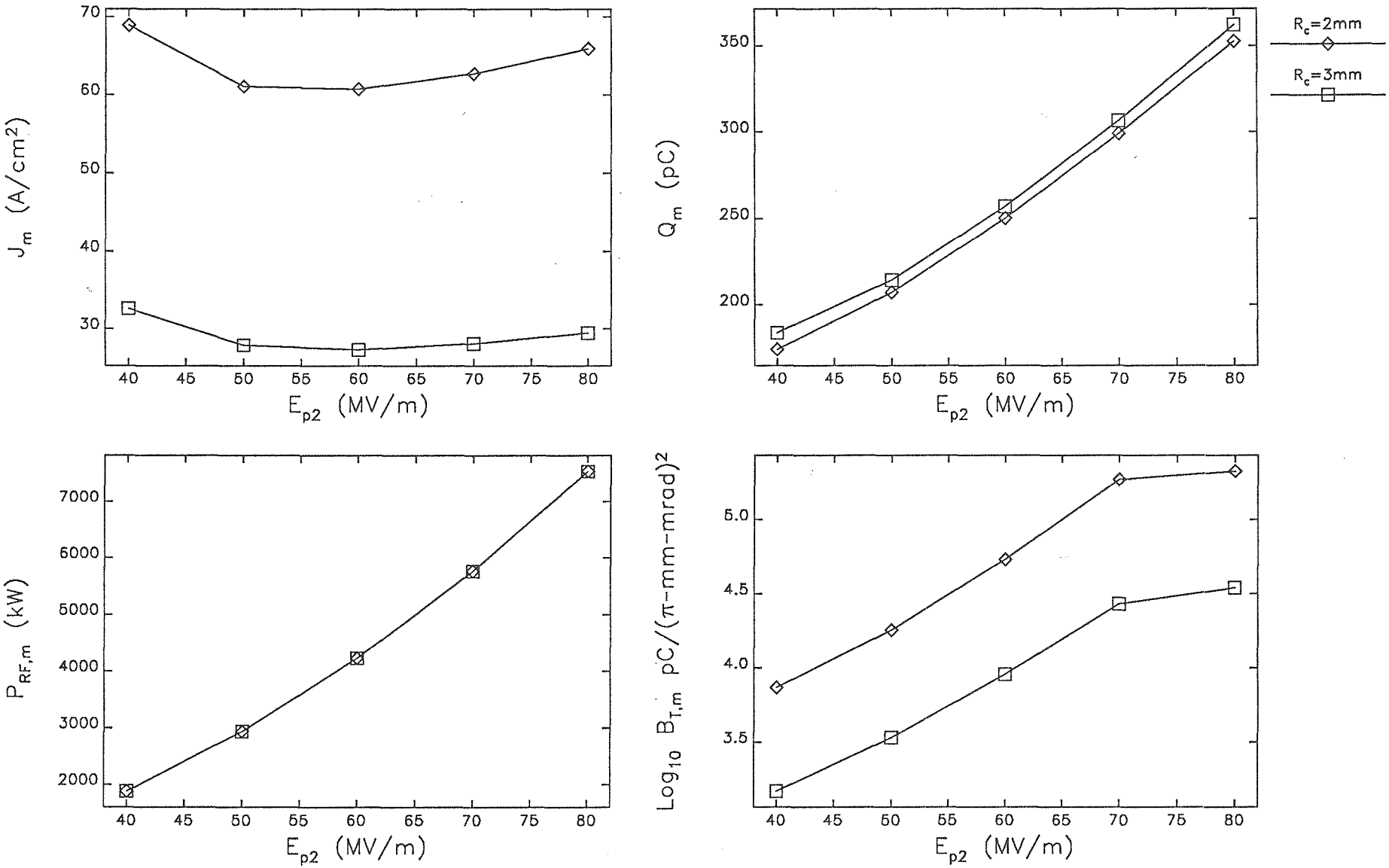
rfgun-calculated Parameters for APS RF Gun for Matched Conditions
J_m (A/cm^2)
E_{p2} (MV/m)
Q_m (pC)
R_c=2mm
R_c=3mm
$P_{RF,m}$ (kW)
Log_{10} $B_{r,m}$ pC/(π-mm-mrad)^2

Figure 5

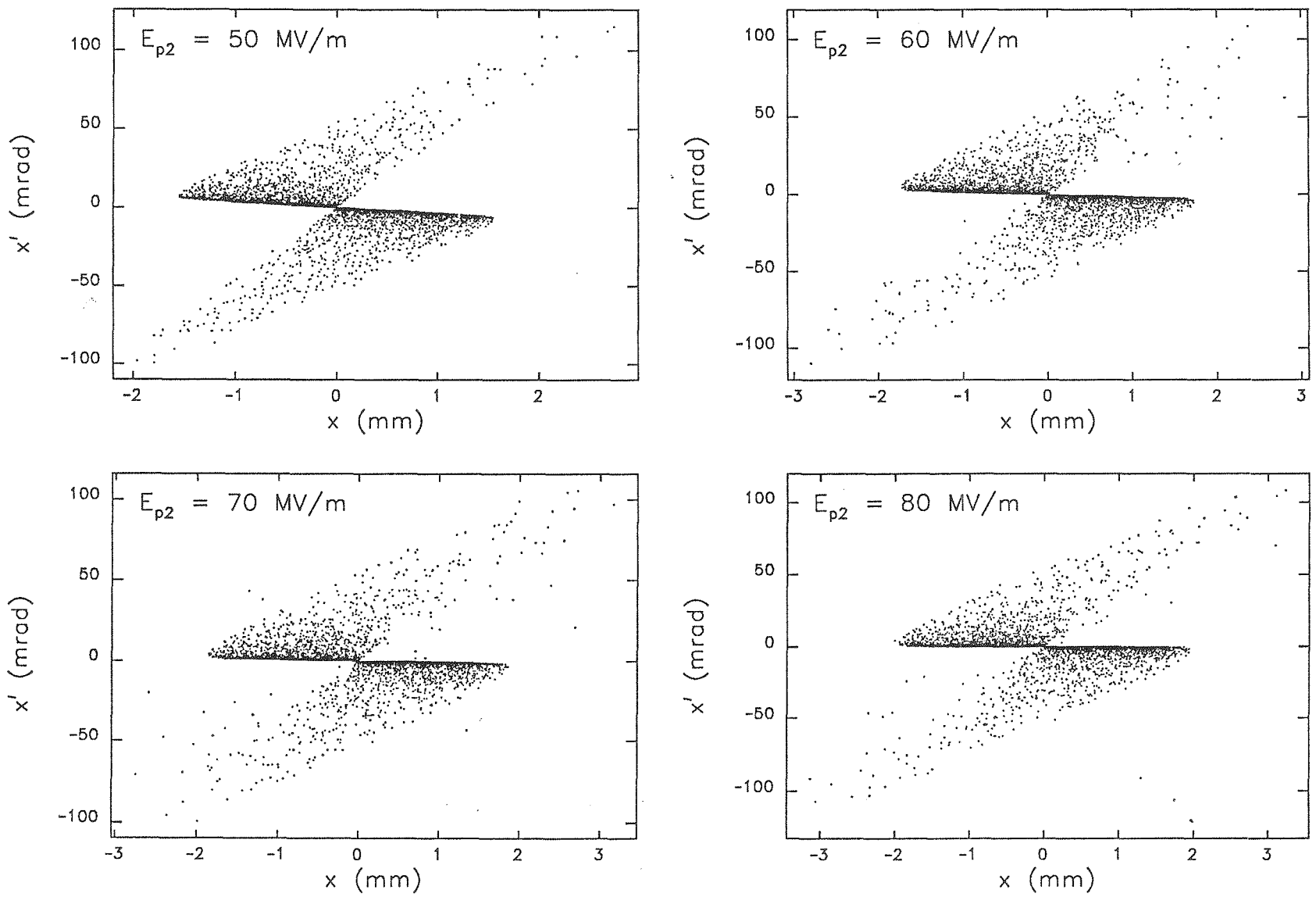
rfgun-Calculated Transverse Phase-Space
E_{p2} = 50 MV/m
E_{p2} = 60 MV/m
E_{p2} = 70 MV/m
E_{p2} = 80 MV/m
x' (mrad)
x (mm)
100
50
0
-50
-100
-3
-2
-1
0
1
2
3

Figure 6

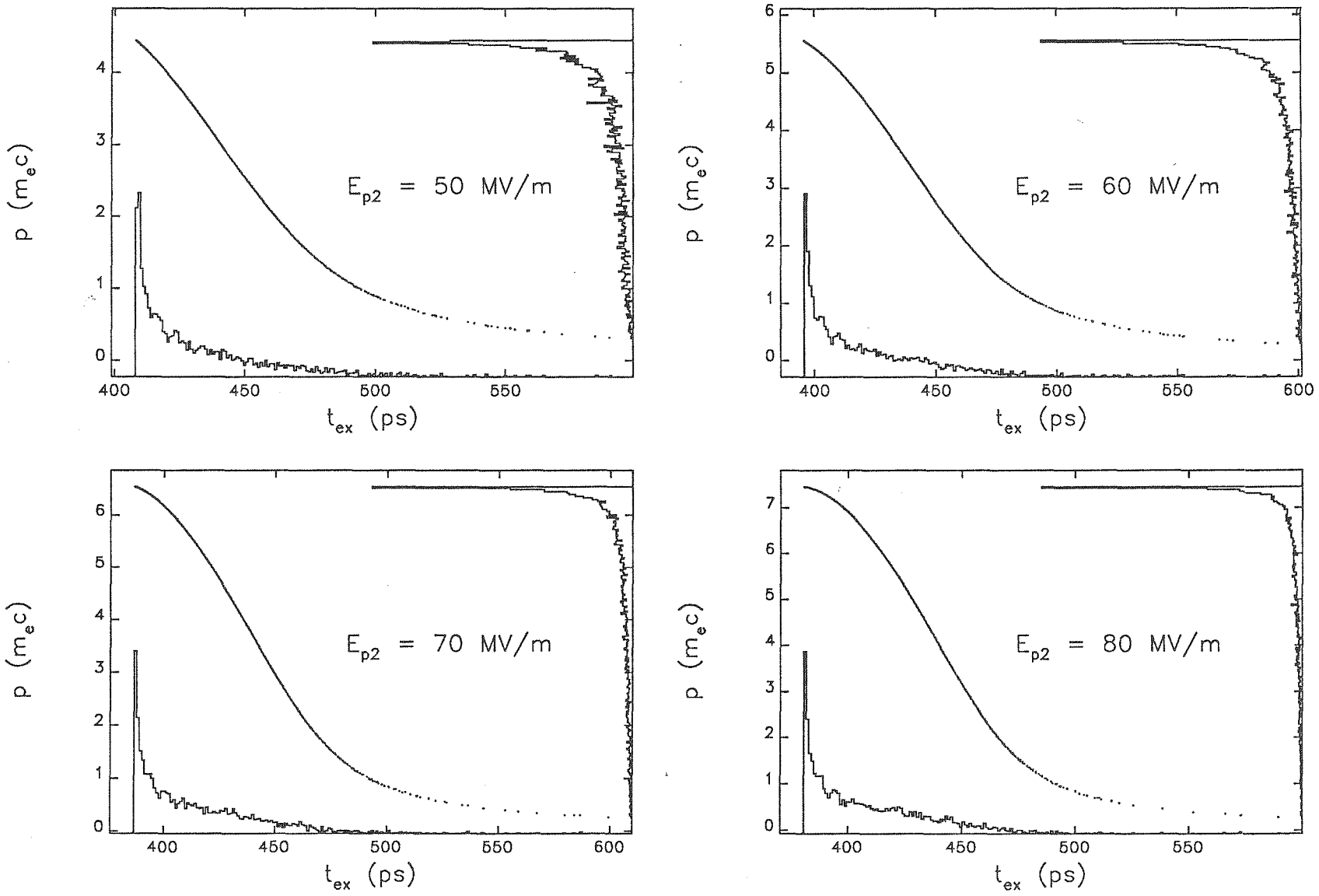
rfgun-Calculated Initial Longitudinal Phase-Space
p (m_e c)
t_ex (ps)
E_p2 = 50 MV/m
E_p2 = 60 MV/m
E_p2 = 70 MV/m
E_p2 = 80 MV/m

Figure 7

Longitudinal Phase-Space after Idealized Magnetic Compression

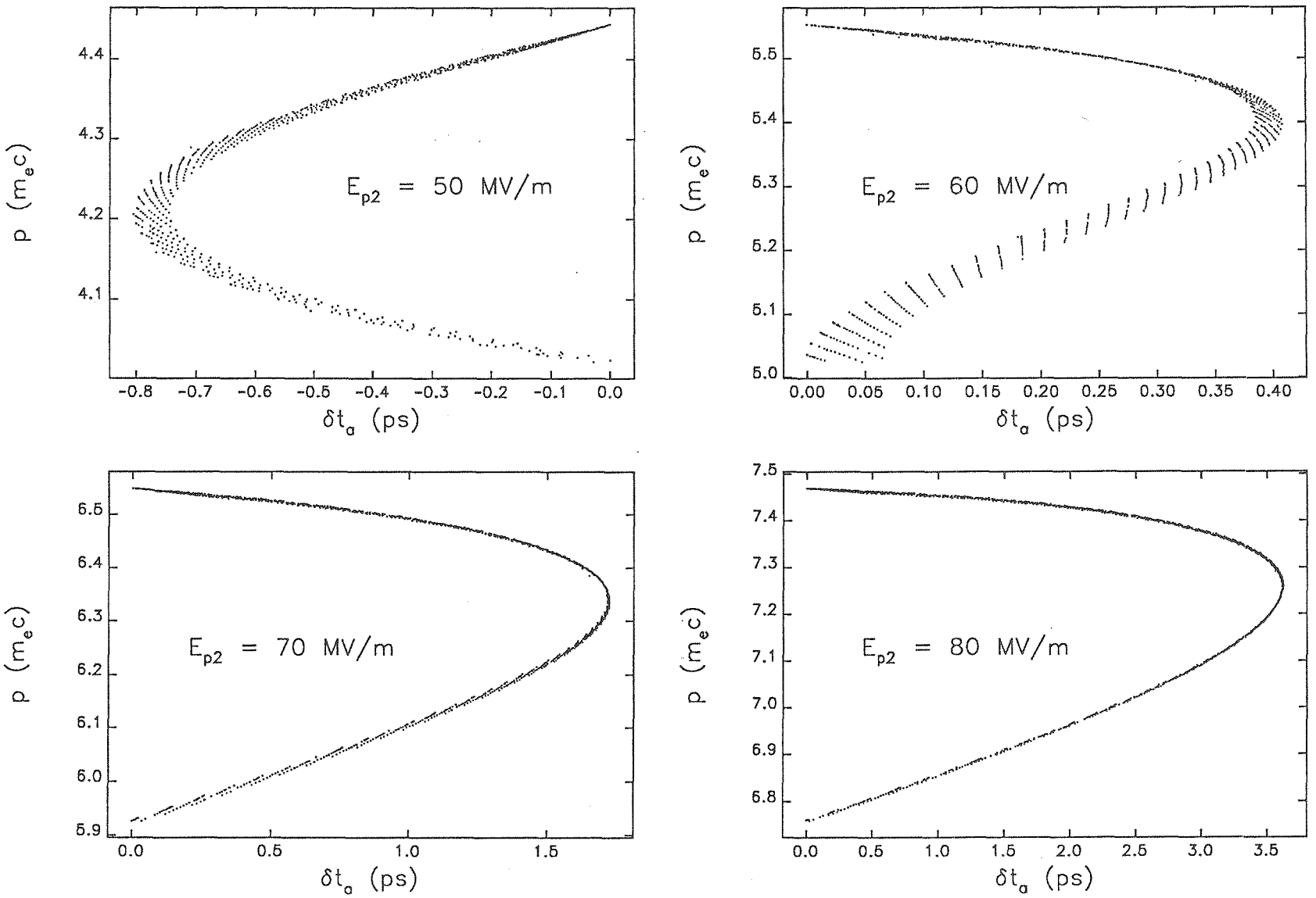

Figure 8

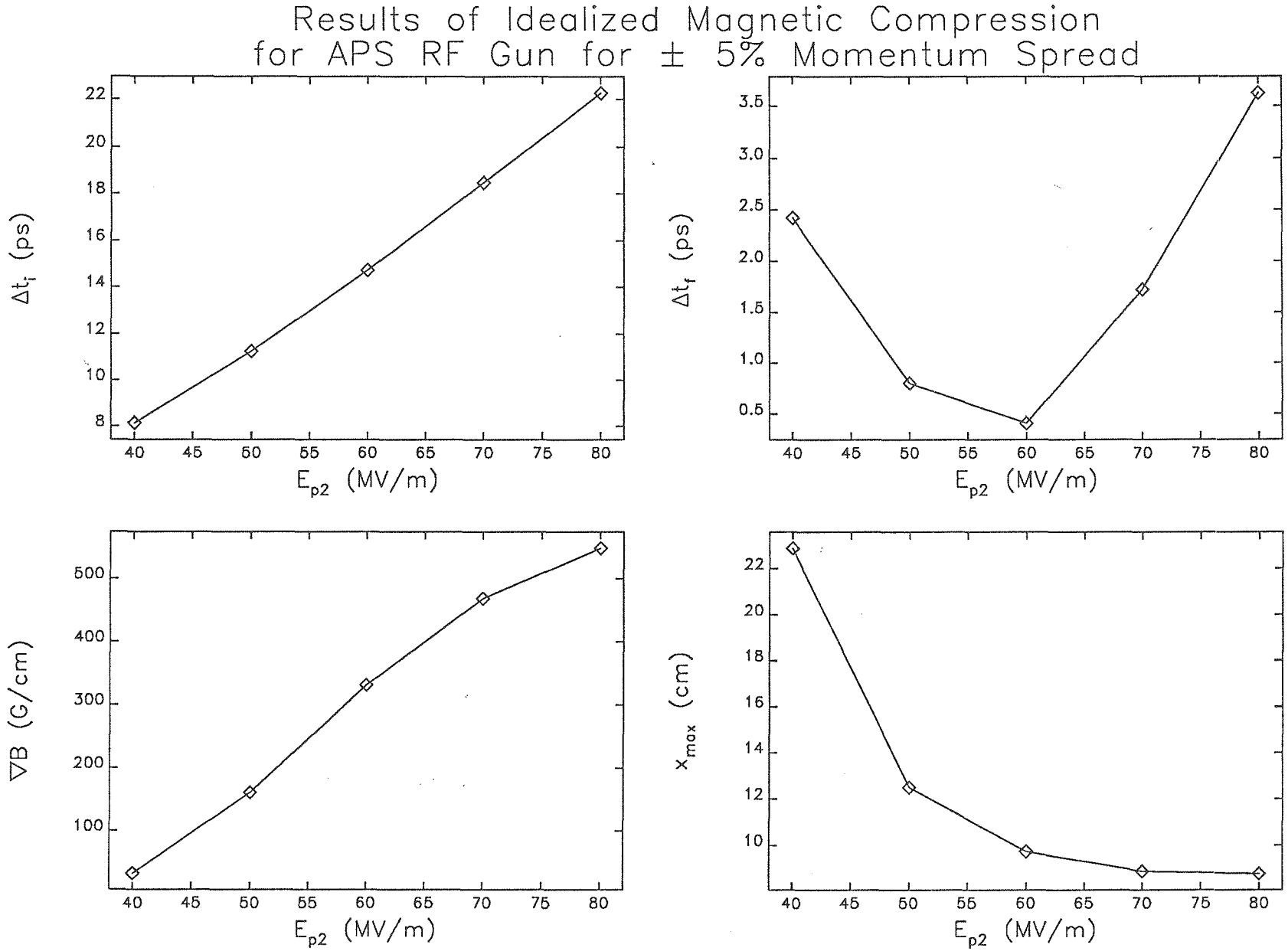
Results of Idealized Magnetic Compression
for APS RF Gun for ± 5% Momentum Spread
Δt_i (ps)
E_{p2} (MV/m)
Δt_f (ps)
E_{p2} (MV/m)
∇B (G/cm)
E_{p2} (MV/m)
x_{max} (cm)
E_{p2} (MV/m)

Figure 9

Table 1: **Geometry of the APS RF Gun**

label	type	z	r	radius	angle
		mm	mm	mm	deg
1	point	0.00	6.00	n/a	n/a
2	point	1.60	13.50	n/a	n/a
3	point	1.60	41.91	n/a	n/a
4	point	6.00	41.91	n/a	n/a
5	arc	6.00	17.27	24.64	0
6	point	30.64	14.818	n/a	n/a
7	arc	28.61	14.818	2.03	270
8	point	27.50	12.788	n/a	n/a
9	arc	27.50	10.588	2.20	180
10	point	25.30	10.08	n/a	n/a
11	arc	30.30	10.08	5.00	270
12	point	32.24	5.08	n/a	n/a
13	point	34.81	5.08	n/a	n/a
14	arc	34.81	10.08	5.00	0
15	point	39.81	10.588	n/a	n/a
16	arc	37.61	10.588	2.20	90
17	point	35.87	12.788	n/a	n/a
18	arc	35.87	14.818	2.03	180
19	point	33.84	17.27	n/a	n/a
20	arc	58.48	17.27	24.64	90
21	arc	58.48	17.27	24.64	0
22	point	83.12	14.818	n/a	n/a
23	arc	81.09	14.818	2.03	270
24	point	79.35	12.788	n/a	n/a
25	arc	79.35	10.588	2.20	180
26	point	77.15	10.08	n/a	n/a
27	arc	82.15	10.08	5.00	270
28	point	84.72	5.08	n/a	n/a
29	point	89.72	5.08	n/a	n/a

Table 2: **Cell Parameters Calculated with URMEL**

quantity	Cell 1	Cell 2	unit
length	3.224	5.248	cm
Q	12500	17042	
Shunt Impedance	1.57	3.63	MΩ
E_{ps}/E_{pi}	1.78	1.75	
E_c/E_{pi}	0.830	n/a	
K_i	0.143	0.212	$mJ/(MV/m)^2$